Double aperture cores are used for wideband transformers up to high frequencies, e.g. made of the materials

SIFERRIT K 1 for matching transformers and balanced mixers up to 250 MHz in antenna feeders or in input circuits of VHF and TV receivers

SIFERRIT U 17 for the same applications up to 500 MHz

SIFERRIT N 30 for lower frequencies and pulse applications

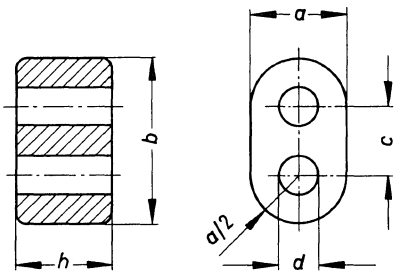

Dimensions in mm

Dimensions *h* mm	*b* mm	*a* mm	*c* mm	*d* mm	Approx. weight g	Material	**Ordering code** (PU: 1000)
14.5_{-1} [1]	14.5_{-1}	$8.5_{-0.5}$	5.85 ± 0.25	$3.4^{+0.8}$	4.0	K 1	B62152-A0001-X001
						U 17	B62152-A0004-X017
$8.3_{-0.6}$ [1]	14.5_{-1}	$8.5_{-0.5}$	5.85 ± 0.25	$3.4^{+0.6}$	2.5	K 12	B62152-A0004-X001
						N 30	B62152-A0004-X030
						U 17	B62152-A0007-X017
$6.2_{-0.5}$ [1]	$7.25_{-0.5}$	$4.2_{-0.4}$	2.9 ± 0.15	$1.7^{+0.3}$	0.4	K 1	B62152-A0007-X001
						N 30	B62152-A0007-X030
$2.5_{-0.3}$	$3.6_{-0.3}$	$2.1_{-0.2}$	1.45 ± 0.1	$0.8^{+0.15}$	0.1	U 17	B62152-A0008-X017
						N 30	B62152-A0008-X030

[1] In accordance with DIN 41 279, shape G

Six aperture cores made of the material SIFERRIT N 22 are preferably used for choke coils to reduce radio interference, e.g. in small motors and switches as well as in high frequency appliances.

Fully wound six aperture cores are also available as complete chokes (see data book 1982/83, "RFI Suppression Components").

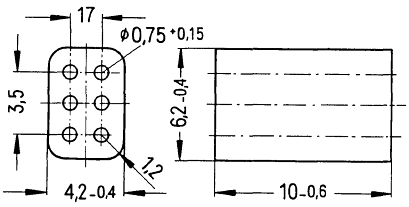

Figure 1

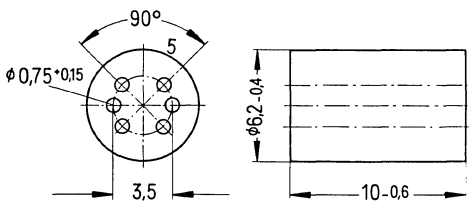

Figure 2

Dimensions in mm

Figure	SIFERRIT material	Approx. weight g	**Ordering code** (PU: 1000)
1	N 22	0.9	B62152-A0005-X022
2	N 22	1.1	B62152-A0006-X022

Impedance characteristics of choke coils
with 2.5 turns at low field strength (< 1 A/m)
(typical values)

SIFERRIT material N 22

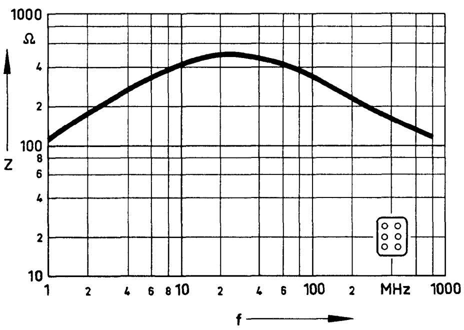

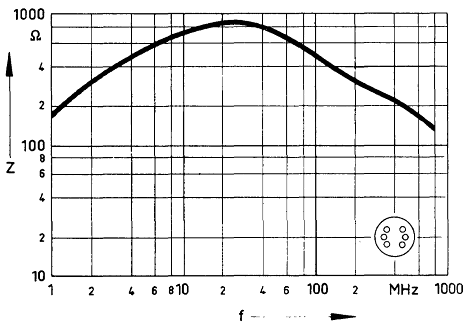

General notes on testing ferrite parts

All Siemens ferrite parts are subjected to severe quality examinations. Our quality assurance program guarantees attaining and maintaining the required Q level throughout every stage of the formation process, i.e. from development via material procurement, production, and testing, up to delivery.

Requirements surpassing this quality level can be met by means of components complying with the CECC System of Quality Assessment. The AQL values for mechanical and electrical characteristics, determined in this system, are particularly severe.
The Siemens ferrite products were granted this licence so that we are capable of supplying pot cores as well as RM cores, made e.g. of the material N 48, meeting the CECC requirements.

Primary and secondary dimensions (major and minor defects) have been determined in accorandance with the CECC Quality Assessment system for examining the dimensions of the ferrite parts. The primary dimensions are examined lotwise with the help of gauges, whereas the secondary dimensions are subject to less severe examinations (see figure below). The gauges used were designed in accordance with DIN 7150, based on a production tolerance and a compensation for wear in accordance with DIN 7151, ISO tolerance series 8.

The following dimensions are to be understood as primary ones, illustrated with a pot core 14 x 8, for example:

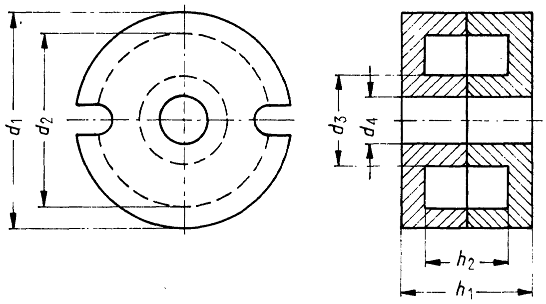

Primary dimensions

in mm	d_1	d_2	d_3	d_4	h_1	h_2
max.	14,2		6,0		8,5	
min		11,6		3,0		5,6

The gauge tolerance for an external diameter of 14.2 mm is e.g. 31 μm, i.e. parts with an external diameter of 14.23 mm can still be evaluated as "good" (utilizing the entire compensation for wear).

SIFERRIT Materials

General material data

Magnetic ferrites are mixed crystals or compounds of ferromagnetic oxides (Fe_2O_3) respectively, with one or several oxides of bivalent metals, such as NiO, MnO, ZnO, MgO, CuO, BaO, CoO. They have a much higher resistivity than metallic materials; the resistivity is 10^0 to 10^5 Ωm compared with 10^{-7} to 10^{-6} Ωm for metallic materials. Contrary to metallic cores, most ferrites have negligible eddy current losses in an alternating magnetic field.

Siemens ferrite cores are well-known under the trademark SIFERRIT®.

General technical data

Tensile strength	approx. 20 N/mm^2
Resistance to compression	approx. 100 N/mm^2
Vickers hardness HV_{15}	approx. 8000 N/mm^2
Modulus of elasticity	approx. 150000 N/mm^2
Heat conductivity	approx. $4 \ldots 7 \cdot 10^{-3}$ J/mm · s · K
Linear expansion coefficient	approx. $7 \ldots 10 \cdot 10^{-6}$/K
Specific heat	approx. 0.7 J/g · K

Resistance to moisture

SIFERRIT is moisture, water and also sea-water-resistant, but can be attacked by several acids in high concentrations.

Resistance to radiation

SIFERRIT materials can be exposed without significant variation ($\Delta L/L \leqq 1$ % for ungapped cores) to the following radiation:

gamma quanta	10^9 rad
quick neutrons	2×10^{20} neutrons/m^2
thermal neutrons	2×10^{22} neutrons/m^2

Shrinkage due to the sintering process

The burning or sintering process produces a considerable shrinkage of the molded body, linearly by 15 % and 40 % by volume. For this reason, often a slight distortion must be accepted, when the cores are not worked after the burning and sintering process. The dimensional tolerances of unworked parts are ±2 to ±3 %.

SIFERRIT Materials

Application survey

Application	Frequency range (MHz)	Flux density low[1]	high
High Q inductors in resonant circuits and filters	... 0,1	x	
	0,2 ... 1,6	x	
	1,5 ... 12	x	
	6 ... 30	x	
High Q inductors in resonant circuits and filters (open)	0,2 ... 1,6	x	
	1,5 ... 12	x	
	6 ... 40	x	
	10 ... 300	x	
Transformers with flat permeability characteristic	... 0,3	x	
Wideband transformers (e.g. antenna transformers for MW, SW, VHF, TV) and pulse transformers for EDP	... 3[2]	x	
	... 5[2]	x	
	... 10	x	
	... 250	x	
	... 400	x	
	... 1000	x	
Power transformers, chokes (e.g. for switched mode power supplies pulse transformers, TV line transformers transducers ignition coils etc.)	... 0,1		x
	... 1		x
	... 1,5	x	x
Attenuators (e.g. wound cylindrical cores, wires with slide-on tubular core)	... 500	x	x
Erase heads	0,2		x
Proximity switches	... 1	x	
	... 2	x	

[1] Low flux density up to approx. 10 mT (Rayleigh range).
[2] Upper frequency limit also depends on core dimensions (in pot core filters also on gap).
[3] Upon request

Material	Type
N 48	Pot, RM, TT cores with air gap
M 33, N 58	
K 1	
K 12	
M 33	Cylindrical cores Tube cores Screw cores Antenna rods, round, slotted
K 1	Cylindrical cores Tube cores Screw cores
K 12	
U 17	
N 48, N 30, T 35, T 38	Pot, RM, X, Q, EP, E cores
N 30	Pot cores
N 30, T 35, T 38	Toroidal cores, EP cores
N 48	Pot cores E cores
M 33	Pot, RM cores
K 1, K 12	Pot cores Double aperture cores
U 17	Cylindrical cores Tube cores
U 60[3])	Double aperture cores
N 27, N 41	U, toroidal, ER, TT cores Pot, PM, RM cores E, EC, CC cores
N 47	RM cores
M 33	Cylindrical cores
N 22	Cylindrical cores, attenuation beads Tube cores Six aperture cores
T 8, T 9, N 22, T 56, T 57	Recording head cores
N 22	Pot cores
M 33	

Material survey

For measuring conditions refer to page 40
For definitions refer to page 15 to 31

		Standard					
SIFERRIT material		K 1	M 33	N 58	N 48	N 27[3]	N 41[3]
Color code		violet	white	–	–	–	–
Initial permeability μ_i		80 ±20%	750 ±20%	1300 ±20%	2000 ±20%	2000 ±20%	3000 ±20%
Optimum frequency range f_{min} f_{max}	MHz MHz	1,5 12	0,2 1,0	0.05 0,6	0,001 0,1	– –	– –
Rel. dissipation factor tan δ/μ_i f_{min} f_{max}	10^{-6}	< 40 < 100	< 12 < 20	< 1,6 < 8	< 0,5 < 2,5	–	–
Curie temperature	°C	> 350	> 200	200	>150	>200	> 230
Coercivity	A/m	500	100	45	20	20	20
Flux density $\hat{B}$ at $\hat{H}$ = 3000 A/m	mT	360	450	420	390	470	470
DC resistivity ρ	Ω m	10^5	5	3	1	1	1
Hysteresis material constant η_B	$\frac{10^{-6}}{mT}$	< 36	< 1,8	< 0,5	< 0,4	< 1,5	< 1,4
Relative temperature coefficient[4] α/μ_i for 20 ... 55 °C/68 ... 131 °F for 20 ... 5 °C/68 ... 41 °F for 20 ... −25 °C/68 ... −13 °F	10^{-6}/K	2...6 1...6 1...6	0,5...2,3 0,5...2,5 0,5...3,0	0,5...1,2 0,5...1,2 0,3...2,0	0,4...1,0 0,4...1,0 0,4...1,5	– – –	– – –
Mean value of α/μ_i for 20 ... 55 °C/68 ... 131 °F	10^{-6}/K	4	1,6	0,9	0,7	3	4
Disaccommodation factor *DF* at 60 °C/140 °F at 20 °C/ 68 °F	10^{-6}	< 35 20	< 12 8	< 6 –	< 4 2	– –	< 6 –
Density	kg/m³	4400	4500	4500	4700	4800	4800
Core shapes		Pot, RM Cylindrical tube threaded toroids double aperture	Pot, RM Cylindrical tube threaded toroids antenna rods	Pot, RM	Pot, RM X TT Q EP	Pot RM TT PM CC E U toroids	Pot RM

[1] Upon request
[2] Perminvarferrite; irreversible changes in quality and permeability occur with strong fields in the core (about > 1500 A/m).
[3] Data for power applications: from pages 89 to 103
[4] For further details refer to pages 48 to 50

materials			Special materials				
N 30	**T 35**	**T 38**	**U 60**[1]	**U 17**[2]	**K 12**	**N 47**[3]	**N 22**
–	–	–	pink	grey	light blue	–	red
4300 ± 20 %	6000 ± 20 %	10000 ± 30 %	8 ± 20 %	10 ± 20 %	24 ± 20 %	1400 ± 20 %	1800 ± 20 %
–	–	–	100 1000	10 220	3 40	–	0,001 0,2
–	–	–	< 2000	< 100 < 1700	< 150 < 600	–	< 2 < 20
> 140	> 130	> 130	> 250	> 500	> 400	> 200	> 145
13	6	4	1000	1500	1200	35	30
380	380	380	110	–	145	430	390
0,5	0,2	0,1	10^5	10^5	10^5	3	1
< 1,4	< 1,4	< 1,4	–	< 27	< 45	< 0,8	< 1,4
– – –	– – –	– – –	– – –	– – –	3 ...14 –0,5...14 –1 ...14	– – –	0,6...1,6 0,6...1,8 07...2,3
1	0,7	0,5	150	40	10	1	0,9
– –	– –	– –	– –	– –	< 50 –	– –	< 7 4
4800	4900	4900	4800	4200	4300	4700	4700
Pot Q, X, TT toroids, double aperture	RM, EP	Pot Q toroids	only upon request	Pot, cylin- drical, tube, threaded double aperture	Pot	Pot RM	Proximity switches, tube, multi- aperture

For further material data (magnetic head cores) refer to page 496.

Material survey

The values for SIFERRIT materials, given in the preceding table, were measured with toroids R 10 (10 mm in diameter) and are, unless otherwise stated, related to room temperature (23 ±3) °C/(73 ±5.4) °F.

Due to reasons of functional efficiency, that data does not generally apply to products of deviating shape and size. Guaranteed values for the individual products are to be found on the appropriate data sheets.

For symbols and definitions refer to page 15 to 31.

The following measuring conditions apply:

		Frequency f	Flux density $\hat{B}$ mT	Other conditions
Initial permeability	μ_i	≦ 10 kHz	≦ 0,1	
Relative loss factor	$\frac{\tan\delta}{\mu_i}$	see table	≦ 0,1	
Curie temperature	ϑ_c	≦ 10 kHz	≦ 0,1	
Peak value of the flux density (≈ saturation flux density $\hat{B}_s$)	B	static		3000 A/m
DC resistivity	ρ			< 10 A/m²
Hysteresis material constant	η_B	$\mu_i \geqq 500$: 10 kHz	1.5 and 3	
		$\mu_i < 500$: 100 kHz	0.3 and 1.2	
Relative temperature coefficient	α/μ_i	≦ 50 kHz	≦ 0,1	for temperature refer to table
Disaccommodation factor	DF	≦ 10 kHz	≦ 0,1	for temperature refer to table

Relative loss factor versus frequency

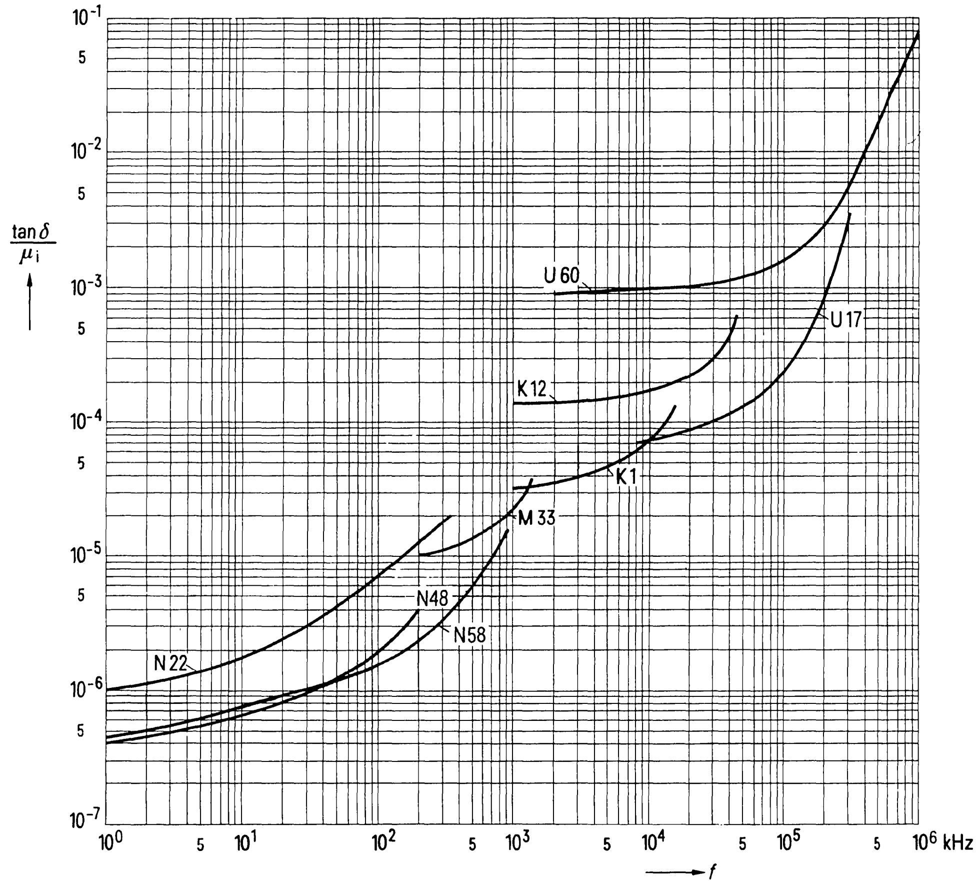

Measured with toroids R 10.
Measuring flux density $\hat{B} \leqq 0.1$ mT

Complex permeability versus frequency

U 17, U 60

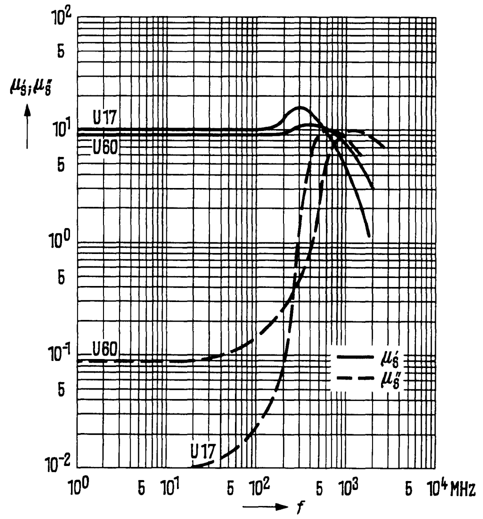

K 12, K 1

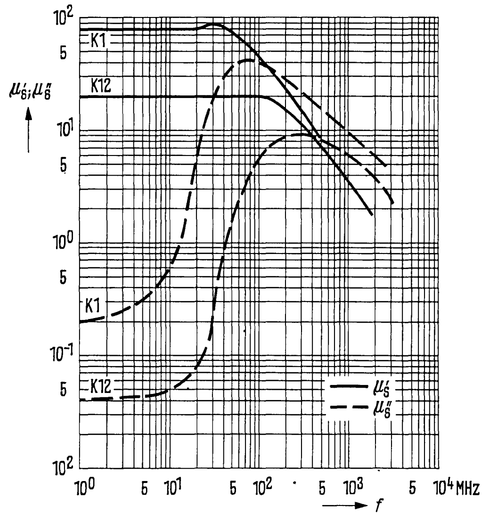

M 33, N 22

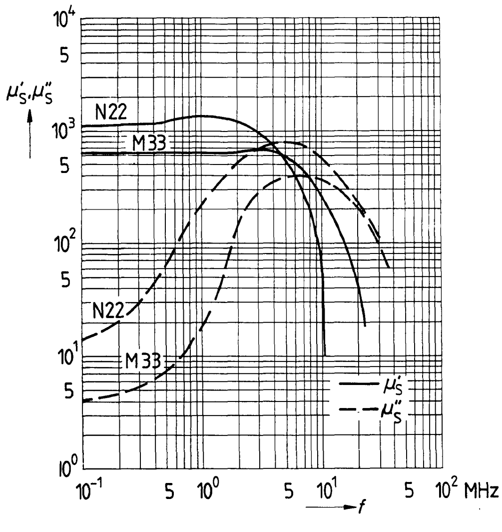

N 48, N 58

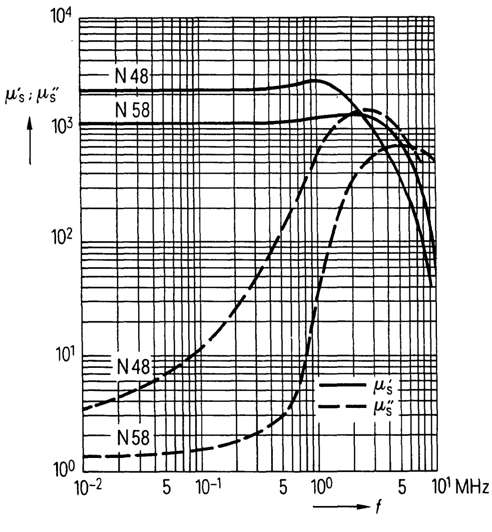

Measured with toroids R 10. Measuring flux density $\hat{B} \leqq 0.1$ mT.

Complex permeability versus frequency

N 27, N 41, N 47

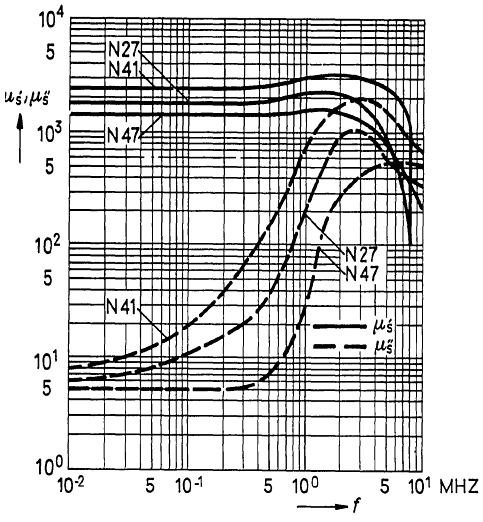

N 30, T 35, T 38

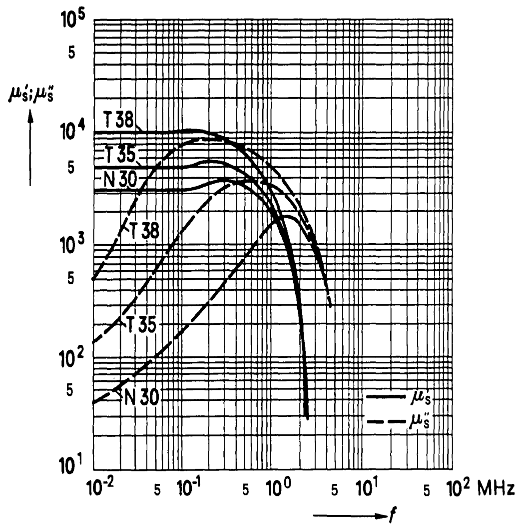

Influence of the core size on the frequency characteristic of the complex permeability, measured with a toroidal core of manganese zinc ferrite Parameter: Core height *h*.

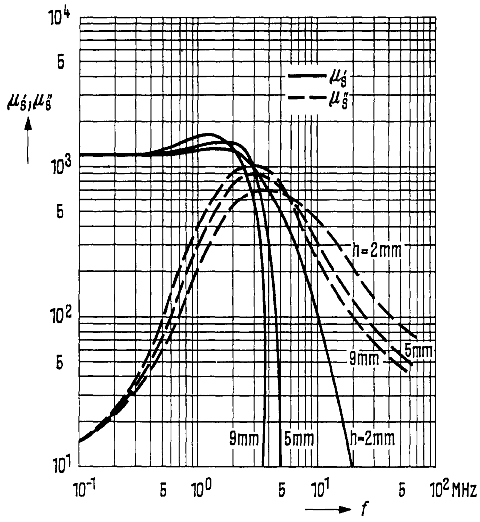

Measured with toroids R 10. Measuring flux density $\hat{B} \leq 0.1$ mT.

Initial permeability and relative loss factor versus temperature

K 12

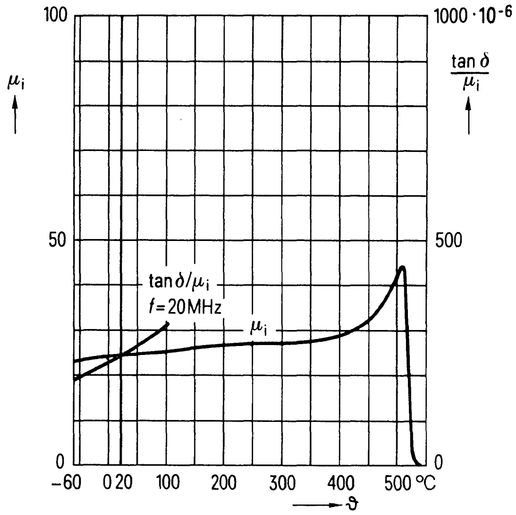

K 1

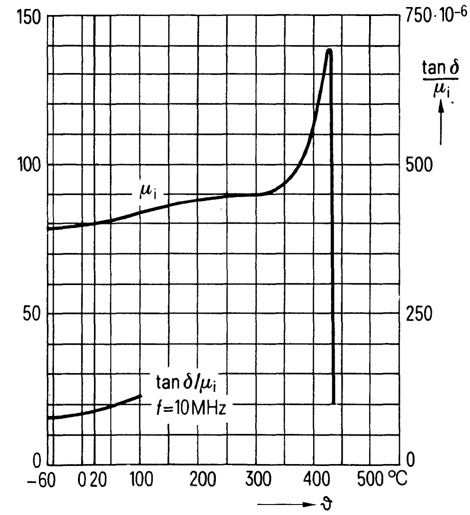

M 33

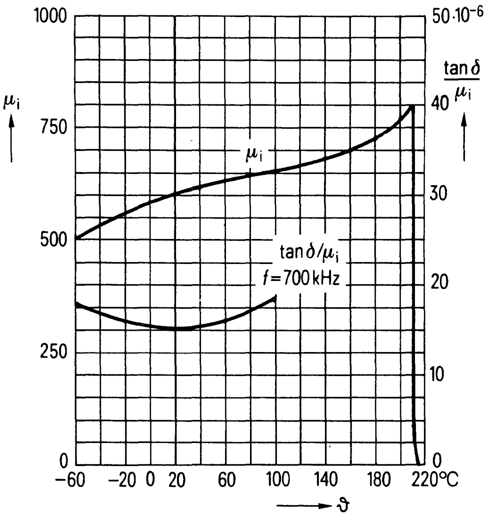

N 22

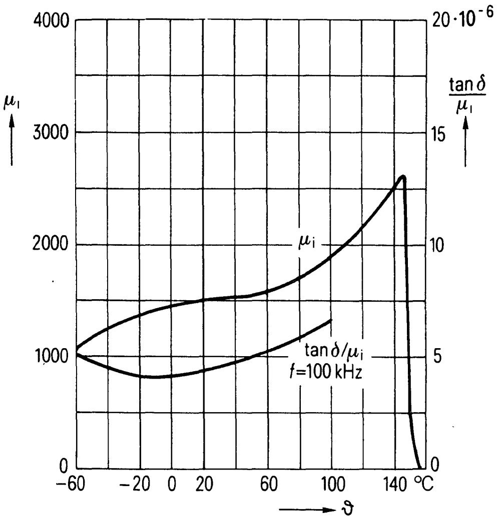

Measuring flux density $\hat{B} \leqq 0.1$ mT.

Initial permeability and relative loss factor versus temperature

N 58

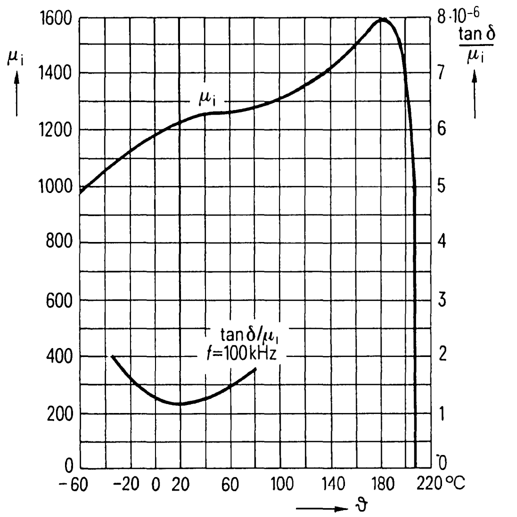

N 48

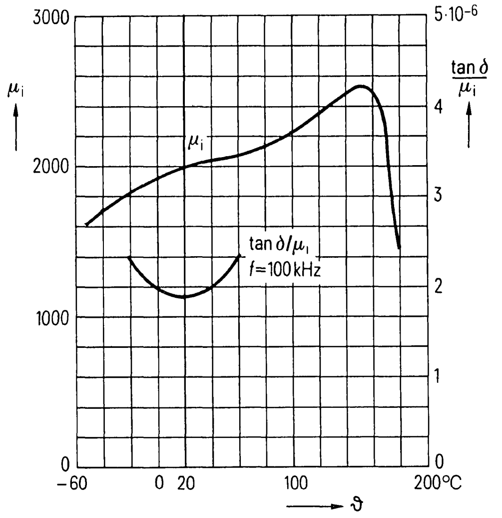

N 30, T 35

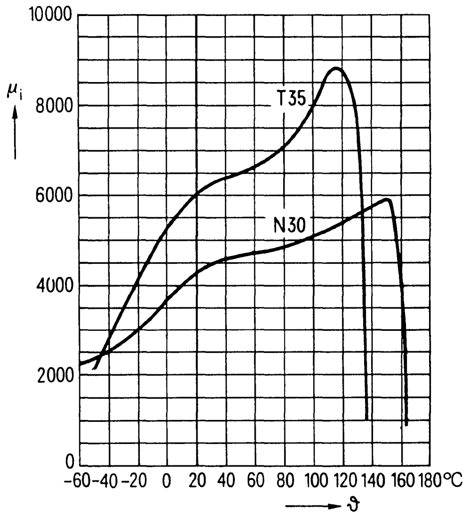

T 38

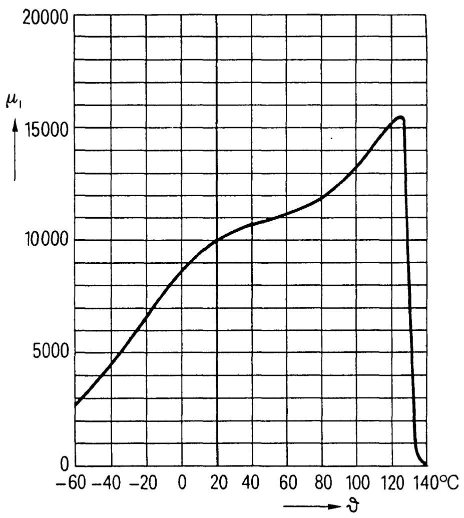

Measuring flux density $\hat{B} \leqq 0.1$ mT.

Initial permeability versus temperature

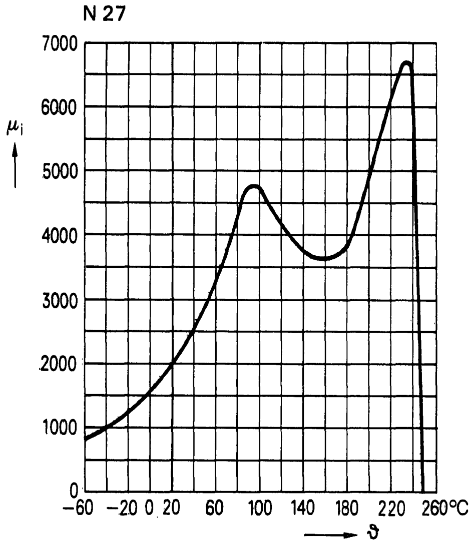

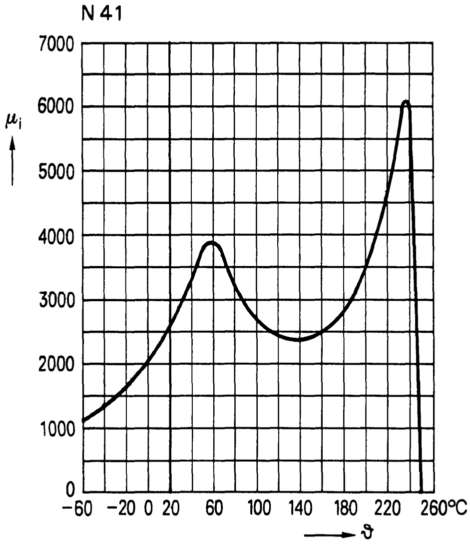

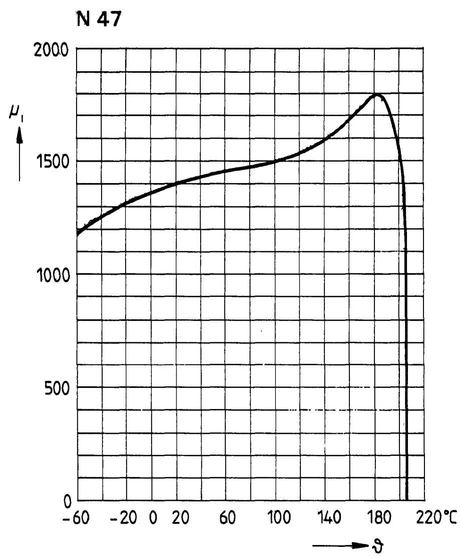

Measuring flux density $\hat{B} \leqq 0.1$ mT.

Variation of initial permeability versus temperature

N 30; $\mu_{i1} \approx 4300$

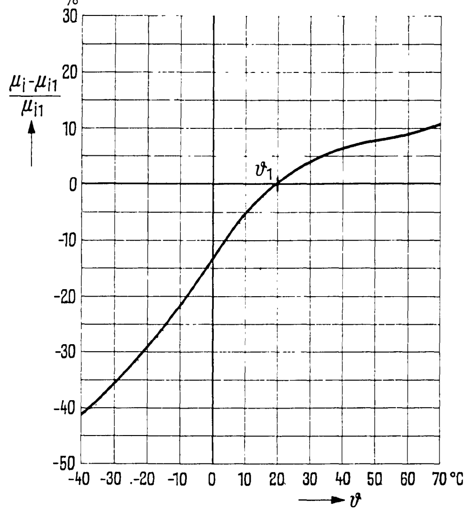

T 35; $\mu_{i1} \approx 6000$

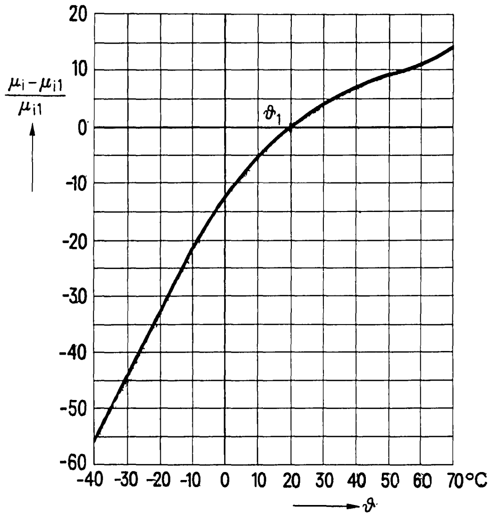

T 38; $\mu_{i1} \approx 10\,000$

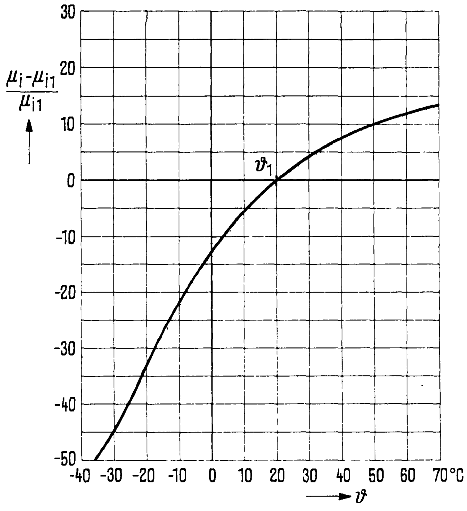

Measuring flux density $\hat{B} \leqq 0.1$ mT.

Permeability factor versus temperature

$$\frac{\alpha}{\mu_i} = \frac{\mu_i - \mu_{i1}}{\mu_i \cdot \mu_{i1}} \cdot \frac{1}{(\vartheta - \vartheta_1)}$$

μ_i at temperature ϑ
μ_{i1} at temperature ϑ_1

$$\frac{\Delta L}{L} [\%] = \frac{\alpha}{\mu_i} [10^{-6}/K] \cdot (\vartheta - \vartheta_1) [K] \cdot \mu_e \cdot 100$$

$$\frac{\Delta L}{L} [\%] = \frac{\mu_i - \mu_{i1}}{\mu_i \cdot \mu_{i1}} \mu_e \cdot 100$$

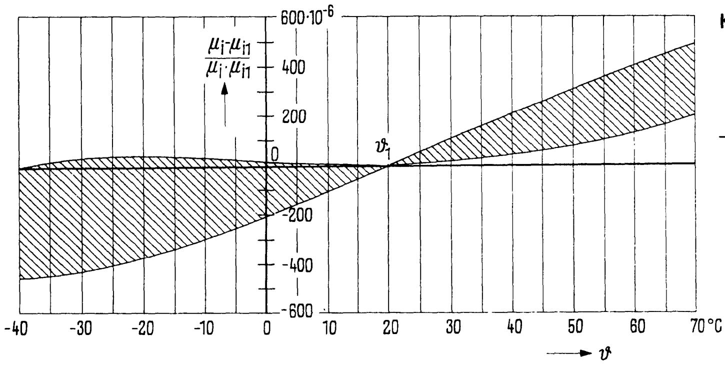

K 12 ($\mu_{i1} \approx 24$)

ϑ °C	α/μ_i 10^{-6}/K
20... 55	3 ...14
20... 5	−0,5...14
20...−25	−1 ...14

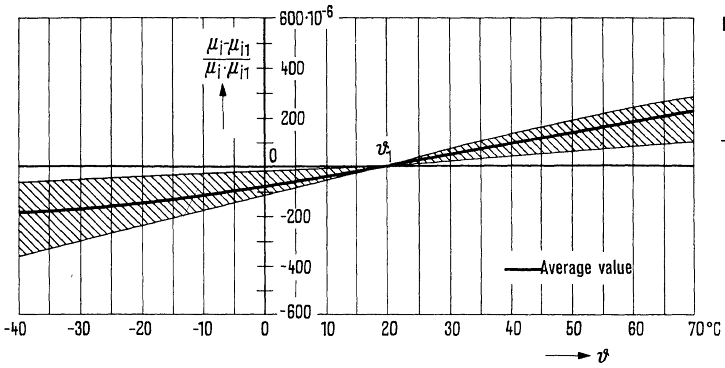

K 1 ($\mu_{i1} \approx 80$)

ϑ °C	α/μ_i 10^{-6}/K
20... 55	2...4 ...6
20... 5	1...4 ...6
20...−25	1...3,5...6

Permeability factor versus temperature

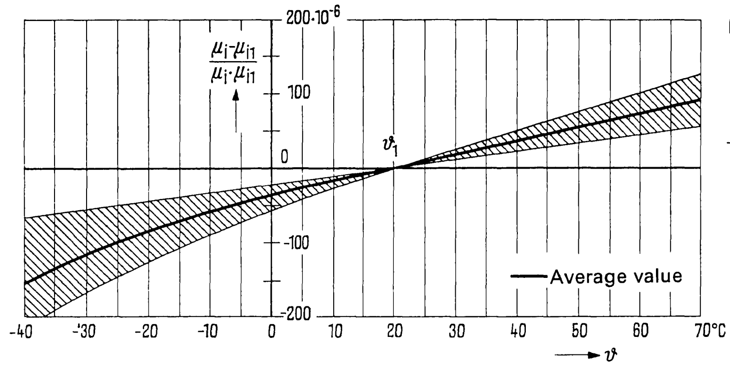

M 33 ($\mu_{i1} \approx 750$)

ϑ °C	α/μ_i 10^{-6}/K
20... 55	0,5...1,6...2,3
20... 5	0,5...1,8...2,5
20...−25	0,5...2,0...3,0

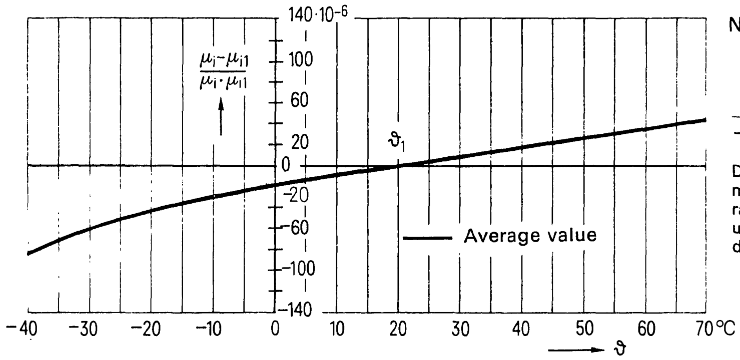

N 58 ($\mu_{i1} \approx 1300$)

ϑ °C	α/μ_i 10^{-6}/K
−20... 70	0,3 ... 2,0

Deviating values for intermediate temperature ranges are only available upon request, since they depend on the core shape.

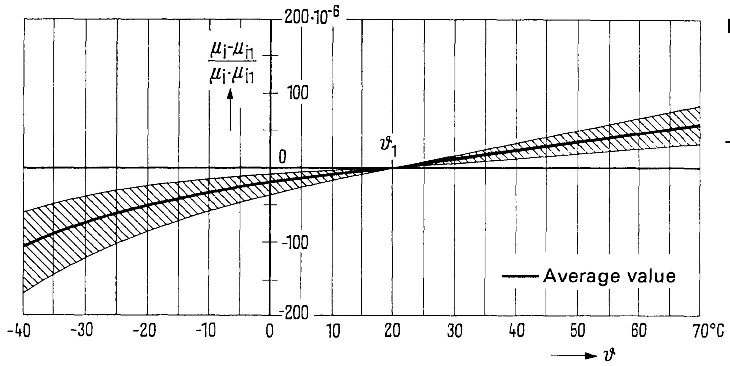

N 22 ($\mu_{i1} \approx 1800$)

ϑ °C	α/μ_i 10^{-6}/K
20... 55	0,6...0,9...1,6
20... 5	0,6...1,0...1,8
20...−25	0,7...1,4...2,3

Permeability factor versus temperature

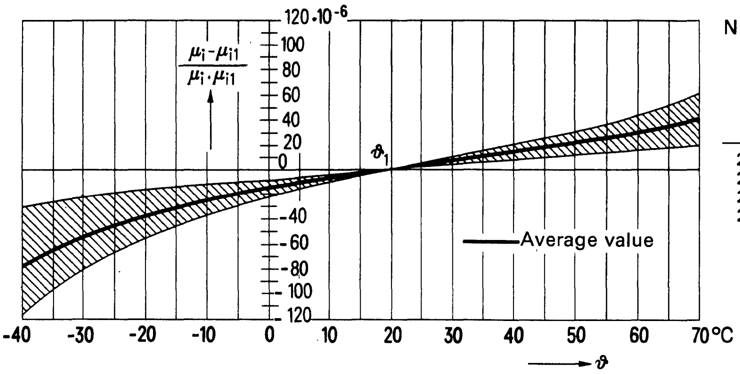

N 48 ($\mu_{i1} \approx 2000$)

ϑ °C	α/μ_i 10^{-6}/K
20... 55	0,4...0,7...1,0[1]
20... 5	0,4...0,7...1,0[1]
20...−25	0,4...0,9...1,5
20...−40	0,6...1,25...2,0

[1] For pot cores greater than 22 mm dia and RM cores greater than RM 8, the α/μ_i value may deviate by up to 1.2×10^{-6}/K.

Static magnetization curves

The static magnetization curves were obtained by the ballistic galvanometer method. The relative total permeability $\mu_{tot} = \frac{1}{\mu_0} \cdot \frac{B_-}{H_-}$ is taken from the curve of normal magnetization (new curve).

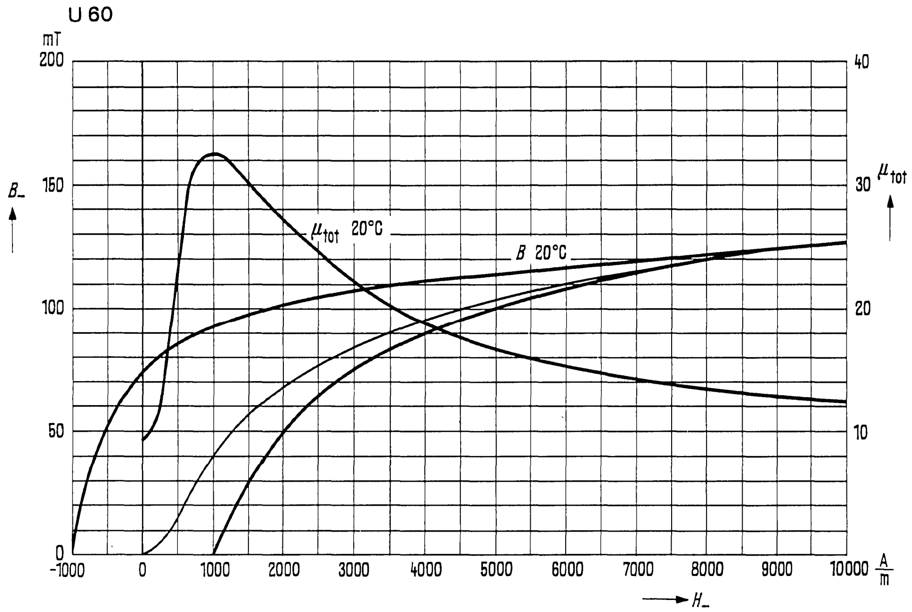

Static magnetization curves

K 12

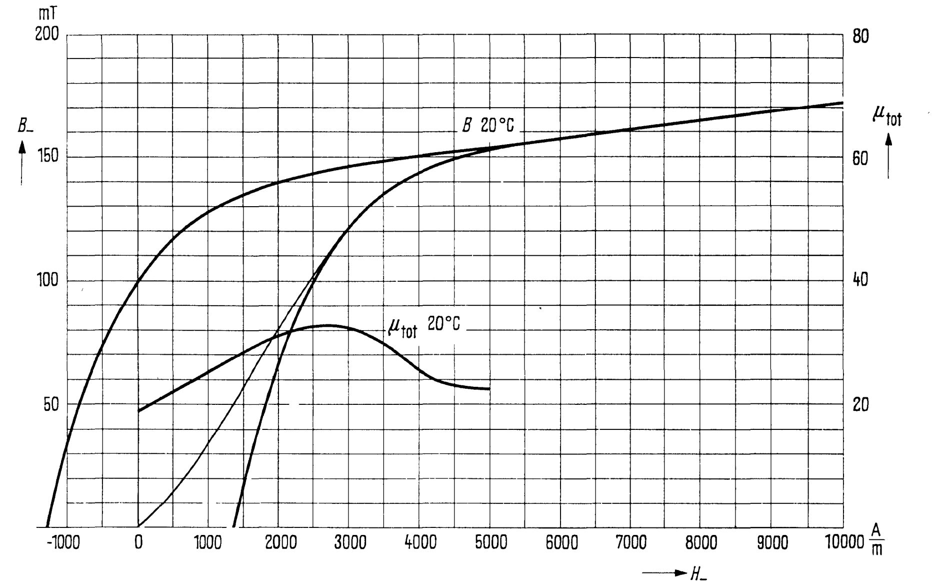

K 1

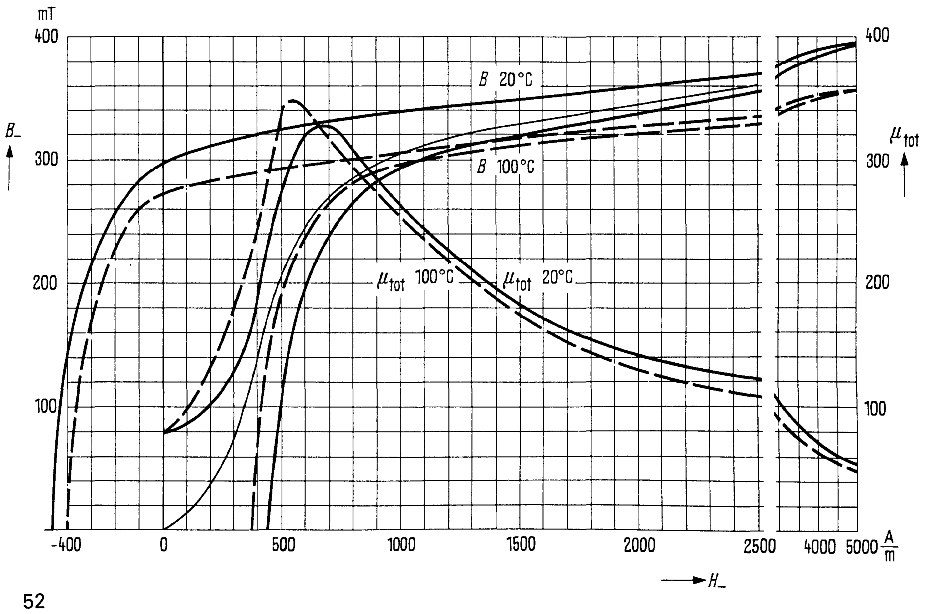

Static magnetization curves

M 33

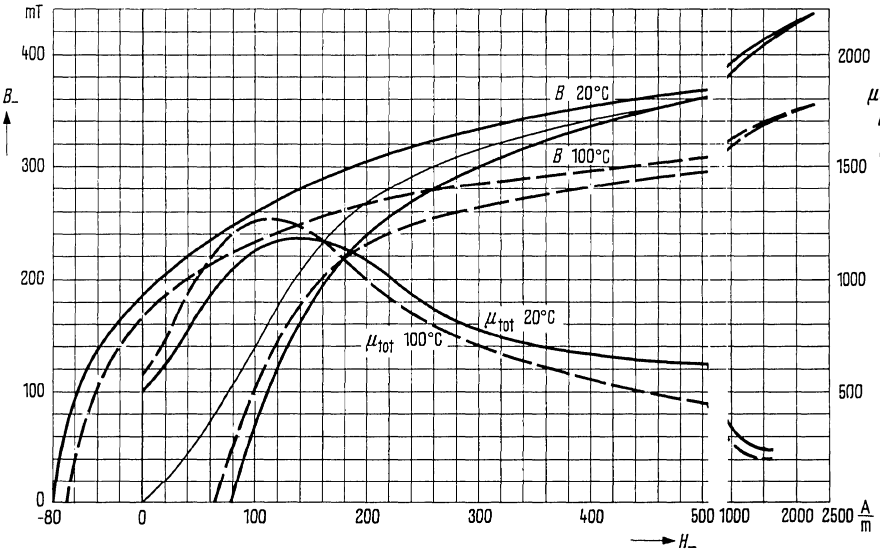

N 58

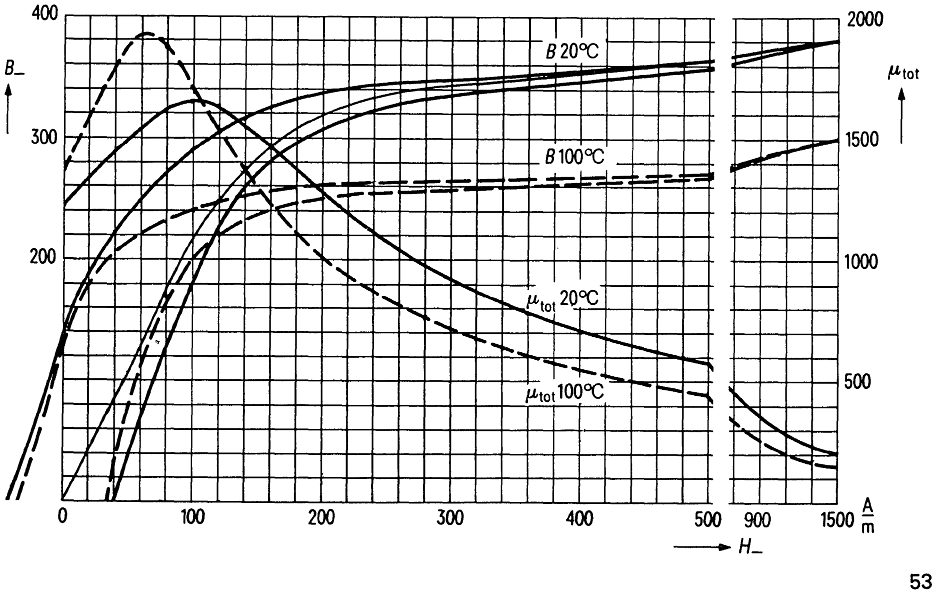

Static magnetization curves

N 47

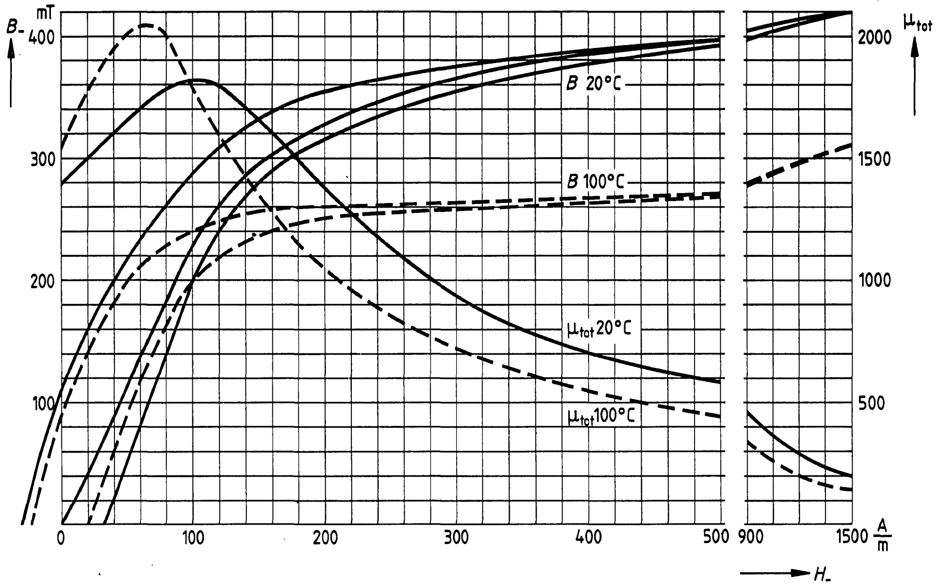

N 22

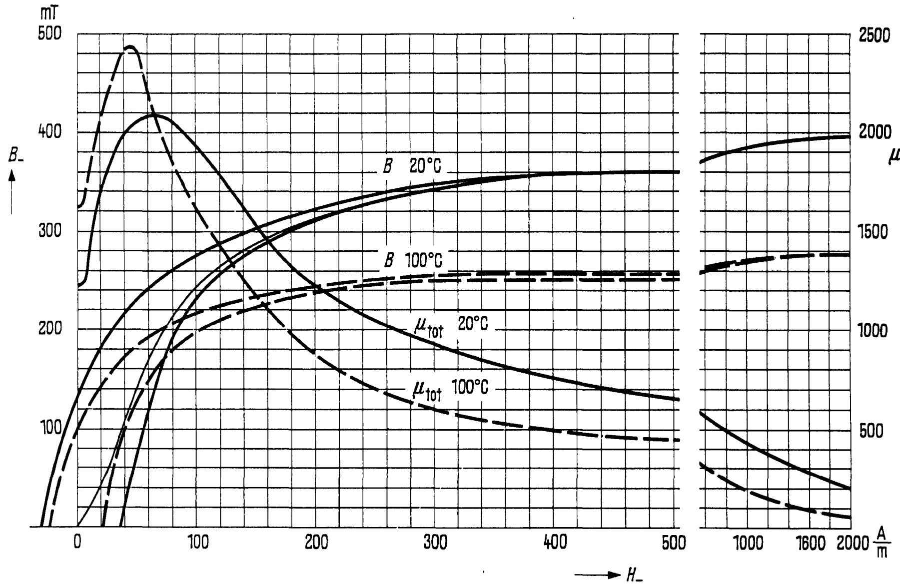

Static magnetization curves

N 48

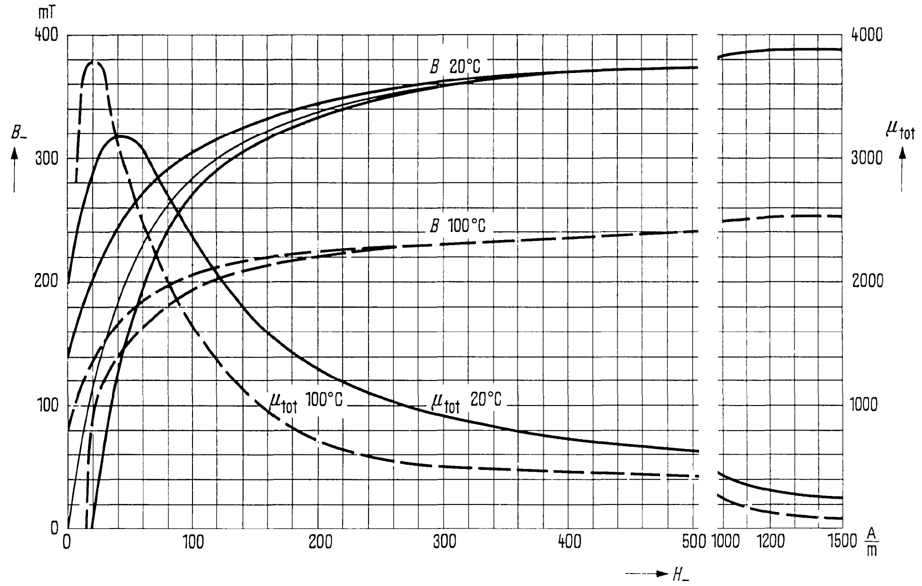

N 27

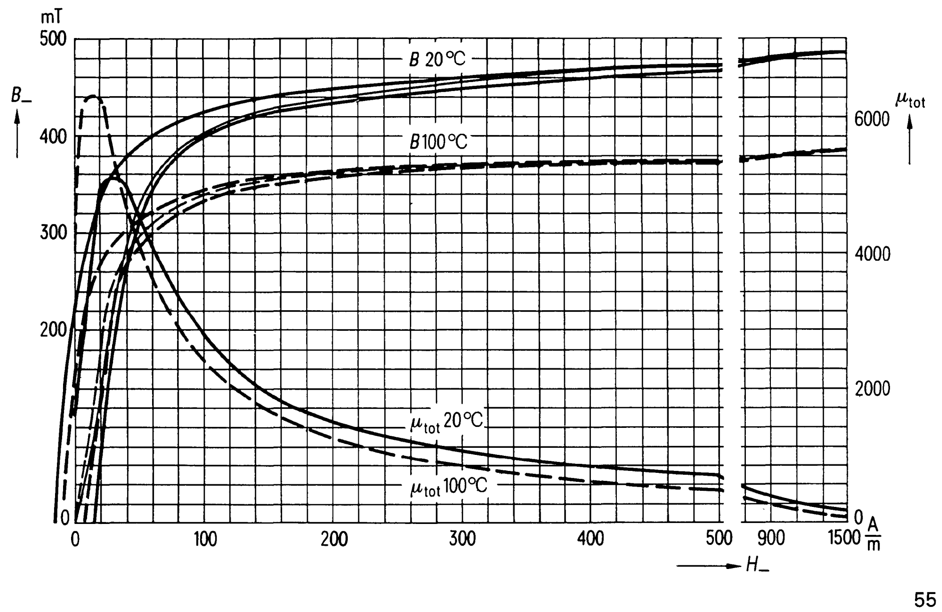

Static magnetization curves

N 41

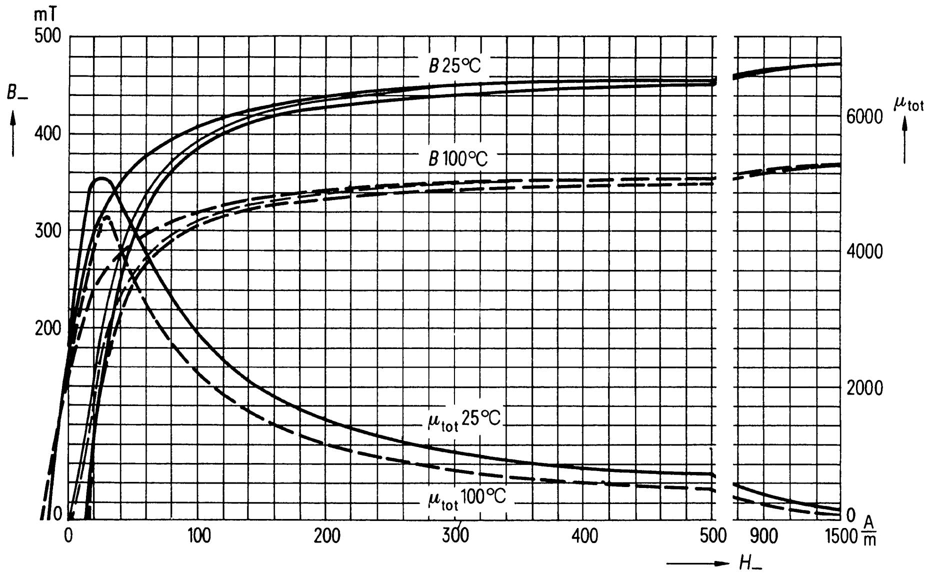

N 30

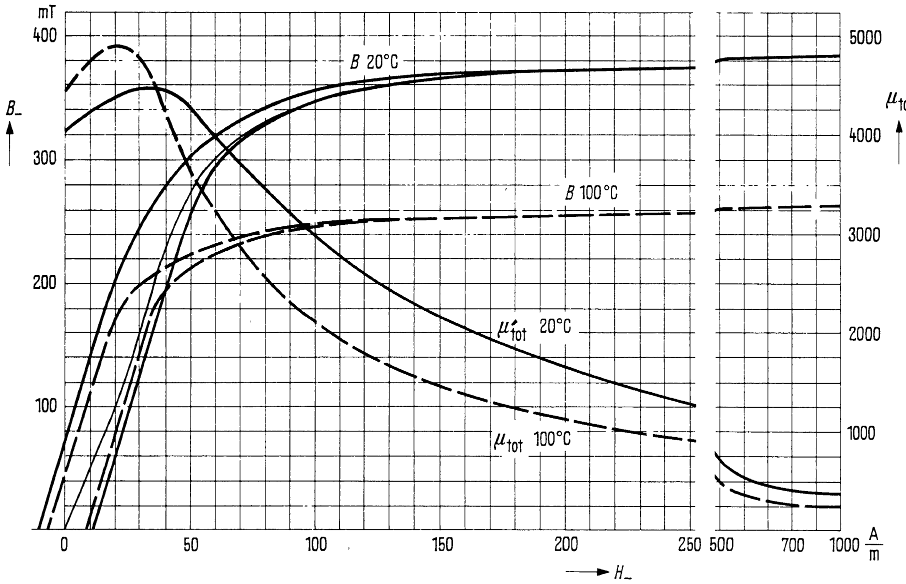

Static magnetization curves

T 35

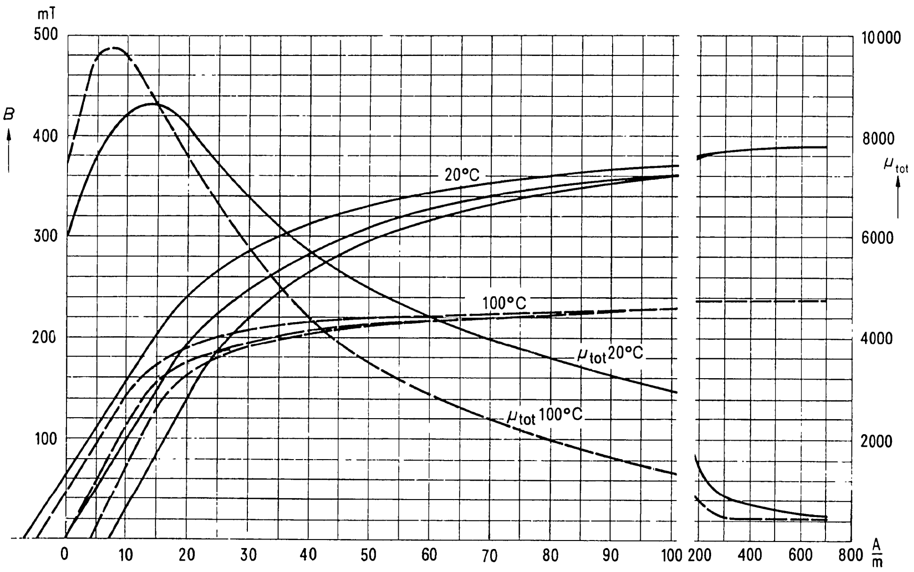

T 38

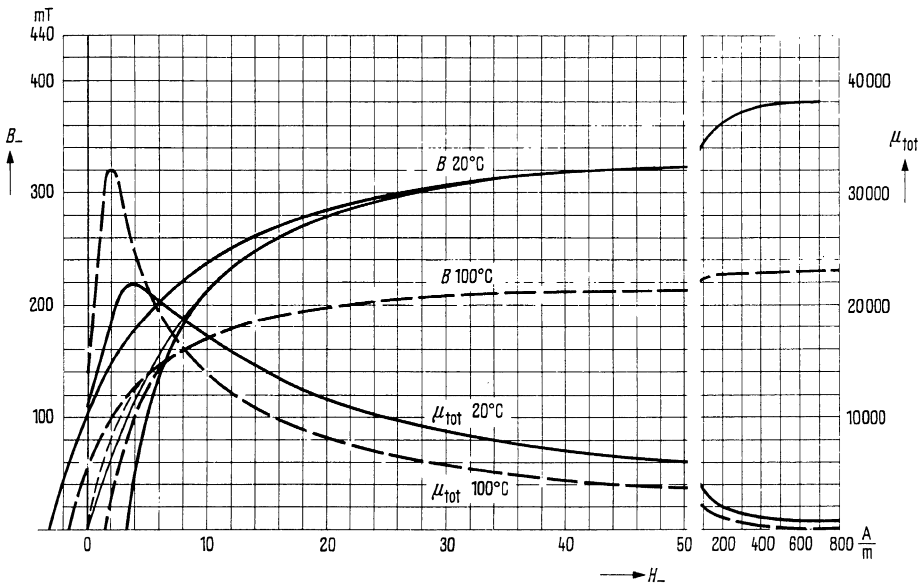

Dynamic magnetization curves

K 1

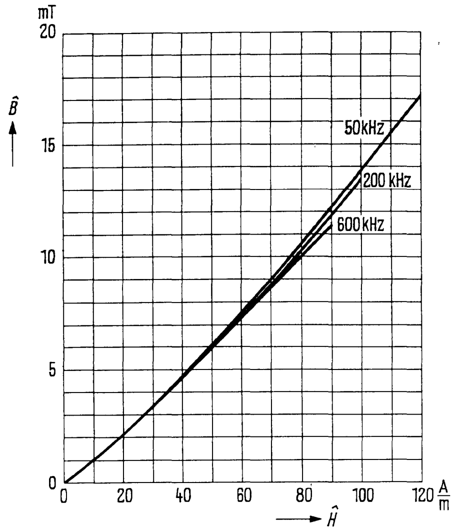

M 33

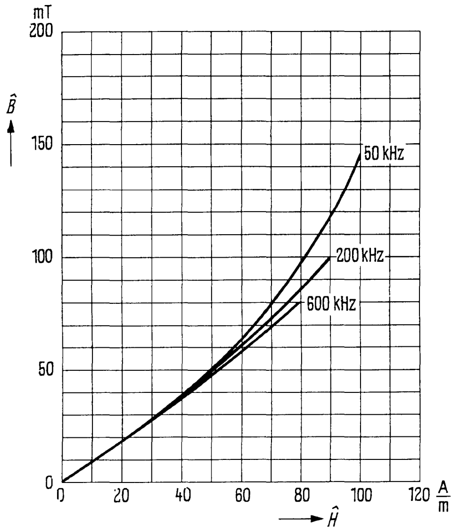

N 22